

Selective optical trapping based on strong plasmonic coupling between gold nanorods and slab

Y. J. Zheng,¹ H. Liu,^{1,a)} S. M. Wang,¹ T. Li,¹ J. X. Cao,¹ L. Li,¹ C. Zhu,¹ Y. Wang,¹ S. N. Zhu,¹ and X. Zhang²

¹National Laboratory of Solid State Microstructures and Department of Physics, Nanjing University, Nanjing 210093, People's Republic of China

²Nanoscale Science and Engineering Center, University of California, 5130 Etcheverry Hall, Berkeley, California 94720-1740, USA

(Received 12 October 2010; accepted 3 February 2011; published online 25 February 2011)

A resonance plasmon mode is formed between a gold nanorod and an infinite slab in infrared range, with local electric field enhancement factor over 40. A strong optical attractive force is exerted on the rod by the slab at resonance frequency. Based on Maxwell stress tensor method and numerical simulations, the optical force was calculated to be over $2.0 \text{ nN}/(\text{mW}/\mu\text{m}^2)$. For a fixed incident wavelength, the enhanced optical force is obtained only for the rods with particular length when the diameter is fixed. This strong optical force could be used as a possible selective optical trapping technique in the future. © 2011 American Institute of Physics. [doi:10.1063/1.3559602]

Since the pioneer work of Ashkin on laser-induced optical trapping,¹ optical trapping, and optical manipulation have experienced remarkable development over the past four decades.^{2,3} In recent years, optical manipulation has revolutionized the field of near-field optical trapping using evanescent wave illumination,⁴ nanometric tips,⁵ or apertures.⁶ Such near-field optical traps make the electric field spatially localized in an area that is much smaller than the diffraction limit. Especially in the past few years, enhancement of near-field optical trapping force by surface plasmon⁷⁻¹² and dielectric resonators^{13,14} have received significant attention. Due to enhancement of the optical trapping force by plasmonic nanostructure, near-field optical traps have developed into an invaluable tool for near-field manipulation and transportation of microsized/nanosized particles. Different branches of nanoscience have benefited from this robust tool.^{15,16}

On the other hand, the plasmonic coupling in metallic nanostructures has also attracted considerable interest. Some hybrid modes and interesting properties can be introduced by the coupling process. Until now, the coupling effect has been widely reported in many nanostructures such as nanospheres,¹⁷ nanoshells,¹⁸ nanorods,¹⁹ and split-ring resonators.^{20,21} Moreover, the coupling between nanostructures and the infinite slab has also been reported.²² Generally, the strong coupling between nanostructures comes from plasmonic resonance, which induces significant enhancement of the local field. As a result, the optical forces between nanostructures are strongly enhanced in this coupling process. The geometric size of the structures plays an important role in resonance plasmon coupling. Therefore, the optical force would also show dependence on geometric size with a high degree of sensitivity. This may possibly provide a method of selective optical trapping techniques. Inspired by these ideas, the strong optical force induced by the plasmonic coupling between gold nanorods and slab was studied based on Maxwell stress tensor method.²³ Furthermore, an alternative

mechanism for surface selective optical trapping was proposed based on the mentioned plasmonic coupling.

The considered configuration is shown in Fig. 1. An isolated gold nanorod was placed on the substrate, which was surrounded by water ($n \sim 1.33$). The substrate included two layers, the upper SiO_2 layer ($n \sim 1.5$) and the bottom gold slab. The size of the square substrate was $1.0 \mu\text{m} \times 1.0 \mu\text{m}$. The thickness h of SiO_2 layer was 10 nm and the thickness b of gold slab was 50 nm. The length l and diameter d of the nanorods are structure parameters.

A commercial software pack (CST MICROWAVE STUDIO) was employed to study the plasmonic coupling properties of the system. The dispersive property of gold was described by the Drudel model with $\omega_p = 1.36 \times 10^{16} \text{ rad/s}$ and $\omega_c = 1.224 \times 10^{14} \text{ rad/s}$.²⁰ The system was illuminated by a plane wave with an electric vector that is linearly polarized parallel to the axis of the nanorod with a normal incidence (intensity of $1.0 \text{ mW}/\mu\text{m}^2$). Periodic boundary conditions were used both in the x and in the y directions. To analyze the resonance of the local field, a probe was placed in the middle layer. The probe detects the local magnetic field between the nanorod and the gold slab. The recorded magnetic

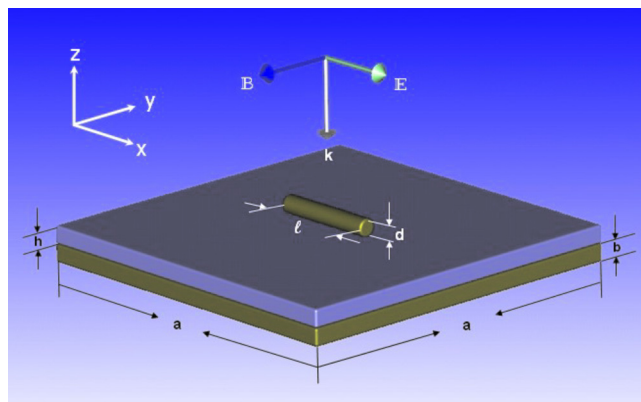


FIG. 1. (Color online) The scheme of plasmonic coupling system: a gold nanorod lay on a gold slab separated by a 10 nm SiO_2 layer. The structure is surrounded by water. A linearly polarized plane wave illuminated normally onto the slab surface with its electric field along the axis of nanorod.

^{a)} Author to whom correspondence should be addressed. Electronic address: liuhui@nju.edu.cn.

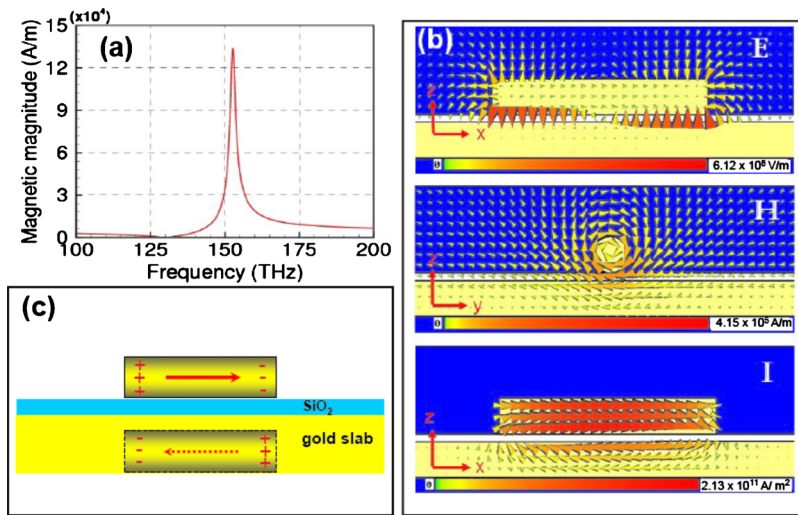


FIG. 2. (Color online) (a) The recorded local magnetic field between the gold nanorod and slab, with the geometrical parameters of the system: $h=10$ nm, $l=300$ nm, $d=50$ nm. (b) Electric field, magnetic field, and electrical current distribution at the resonance frequency. (c) Equivalent picture of the plasmonic coupling between the nanorod and the slab: nanorod interactions with its inverse image inside the slab.

field when the frequency of the incident wave was swept from 100 to 200 THz is plotted in Fig. 2(b). A pronounced resonance peak was recorded at 152.7 THz, where the local field was remarkably amplified by more than a factor of 40 in magnitude compared with the incident wave. At the resonant frequency, the local field and the current were obtained from simulation data with the results shown in Fig. 2(b). At resonance, the electrons inside the rod were excited by an incident electric field, making them oscillate along the axis of the field. This caused the nanorod to behave like an oscillating electric dipole. The electric field of the dipole induced an opposing charge in the surface of the slab, as shown in Fig. 2(b). As a result, strong coupling happens between the nanorod and the slab, which lead to high field enhancement⁷ and significant enhancement of the optical force compared with that of the uncoupled case. This coupling between the nanorod and the slab can also be perceived as the coupling between the nanorod and its reverse image inside the slab [Fig. 2(c)]. The charge induced inside the “image” is always opposite that of the nanorod. Therefore, the near-field coulomb interaction between the nanorod and its inverse “image” is always that of attraction.

The optical force can be greatly enhanced only when the resonance frequency of the nanorod is consistent with the incident frequency. However, the plasmon resonance properties of the nanorod are extremely sensitive to its geometric size. In this study, the dependence of the resonance mode on the length and diameter of the nanorod were investigated. The results show that with increases in l and d , the resonant frequency exhibited a distinct redshift and a blueshift, re-

spectively, as shown in Figs. 3(a) and 3(b). Therefore, the optical force on nanorods would be significantly sensitive to their length and diameter with a fixed incident frequency.

The model employed to calculate the optical force induced by the plasmonic coupling between the nanorod and the slab was based on Maxwell stress tensor method. The electric and magnetic fields could be obtained directly from the simulation data. Evaluating Maxwell stress tensor $\vec{T} = \epsilon \mathbf{E}\mathbf{E} + \mu \mathbf{H}\mathbf{H} - \vec{\mathbf{I}}/2 \cdot (\epsilon |E|^2 + \mu |H|^2)$ and integrating it over the closed surface of the nanorod, the time-averaged optical force can be obtained. This is done using the following equation: $\langle \mathbf{F} \rangle = \langle \oint_V \vec{T} d\mathbf{S} \rangle$, where $\vec{\mathbf{I}}$ is the unit tensor, ϵ is the permittivity of the medium, μ is the permeability of the medium, and $\langle \cdot \rangle$ denotes the time-averaged factor. When there is mirror symmetry in both x and y directions, the net optical force exerted on the nanorod along the x and the y direction should be equal to zero. Therefore, only the vertical component of the force F_z needs to be considered.

Due to the plasmonic coupling, a strong optical force could be generated at the resonance frequency. To confirm this expectation, the optical force exerted on the nanorod under different incident frequencies was calculated. The optical force was greatly enhanced around the resonance frequency. At the resonant frequency, the maximum value of the optical force can reach 2058 pN with an incident intensity of $1.0 \text{ mW}/\mu\text{m}^2$. When the frequency shifted away from the resonance, the force decreased rapidly as shown in Fig. 4(a). The negative value indicates that the direction of optical

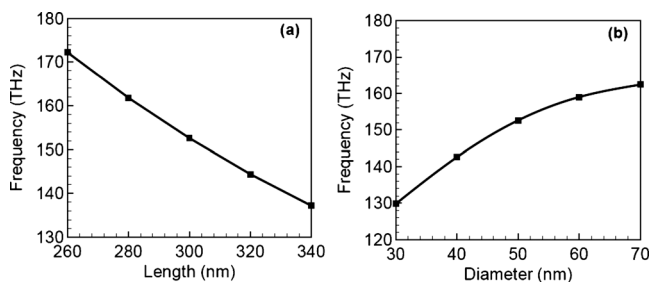


FIG. 3. Resonance frequencies dependent on the geometric size of the nanorod. (a) Length of the nanorods range from 260 to 340 nm with diameter fixed at 50 nm. (b) Diameter of the nanorods range from 30 to 70 nm with length fixed at 300 nm.

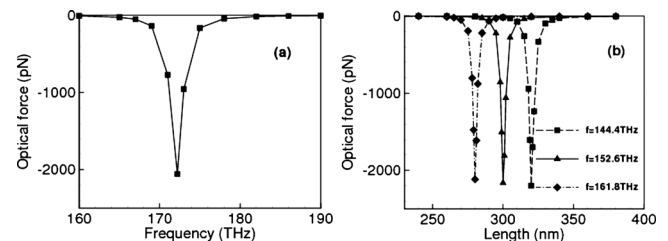


FIG. 4. (a) Spectra of the optical force as a function of the incident frequency, with the geometrical parameters of the system: $h=10$ nm, $l=260$ nm, $d=50$ nm, and the incident intensity of $1.0 \text{ mW}/\mu\text{m}^2$. (b) Spectra of the optical force as a function of length of nanorod for three incident wave with frequency $f=144.4$ THz, 152.6 THz, and 161.8 THz, with the geometrical parameters of the system: $h=10$ nm, $d=50$ nm, and the incident intensity of $1.0 \text{ mW}/\mu\text{m}^2$.

force was downward. The total optical force is composed of two parts: the radiation force from the incident wave and the coupling force from the slab. At the resonance frequency, the optical force due to plasmonic coupling was much stronger than the nonresonance radiation force. As a result, the optical force on the nanorod was governed by plasmonic coupling between the nanorod and the slab, which resulted in a greatly enhanced attractive force toward the surface. This sensitive dependence of the optical force to frequency is useful for selective trapping applications.

For a quantitative analysis of the mechanism of surface selective optical trapping, we studied the dependence of the enhanced optical force by plasmon coupling on the parameters of the nanorod with fixed frequencies. In our simulations, the length of the nanorods was increased from 225 to 375 nm with their diameter unchanged at 50 nm. Using three different incident frequencies, 144.4, 152.6, and 162.8 THz, the dependence of the optical forces on l are described by the three curves in Fig. 4(b). The results show that for these three incident frequencies, the optical force curves exhibit resonance ditches at three different lengths, namely 320 nm, 300 nm, and 280 nm, for 144.4 THz, 152.6 THz, and 162.8 THz, respectively. These ditches in the curves come from resonance coupling. For different incident frequencies, resonance occurred for different lengths of nanorods. Therefore, different resonance optical forces were produced for nanorods with different lengths. This length-dependence of the optical force is useful in selective trapping. The length of the nanorod plays an important role in the application of nanophotonics, nanomachines, and nanomedicine. However, in a practical chemical action of a fabrication process, the length of the nanorods is hard to control precisely and uniformly.²⁴ The use of the aforementioned length-dependent optical force is possible to select the nanorods with specified length.

The plasmonic coupling-based selective trapping system proposed here has several possible advantages compared with previously reported techniques. First, the configuration is significantly simpler. The process only requires depositing a gold film and a layer of SiO₂ on the substrate, thus eliminating the need for complicated nanopatterns. Second, this configuration provides better utilization of available laser power because it benefits from the strong plasmonic coupling in the structure, which greatly reduces the operating power and avoids possible damage to the trapped nanorods. Moreover, aside from tuning optical force through changing the frequency of the incident light, the optical force is also tunable through changes in the incident polarization direction. In our system, the plasmonic coupling was excited by the component of electric field along the axis of the nanorod. By changing the angle between the incident electric field and the axis of the nanorod, the electric field along the axis of the rod was changed continually. As a result, the magnitude of the optical coupling force could be precisely tuned by rotating the polarization of the incident light, leading to a conve-

nient and precise manipulation of the nanorods.

In summary, our study investigated the plasmonic coupling-induced strong optical force between the gold nanorod and the slab. A localized plasmonic resonance mode could be established between the nanorod and the slab. With an incident intensity of 1.0 mW/ μm^2 , the optical force could reach several nanonewtons at resonance frequency. With a definite incident frequency, the optical force exhibited sensitive dependence on the length of the nanorod with a fixed diameter. This provides a possible way to perform a surface-selective trapping technique. These remarkable properties, together with the ease of fabrication of the proposed structure, make microsystems/nanosystems for optical manipulation of nanosized objects at the surface of a chip very promising.

This work was supported by the National Natural Science Foundation of China (Grant Nos. 11074119, 11021403, 10874081, and 60990320), and by the National Key Projects for Basic Researches of China (Grant No. 2010CB630703).

¹A. Ashkin, *Phys. Rev. Lett.* **24**, 156 (1970).

²D. G. Grier, *Nature (London)* **424**, 810 (2003).

³M. Dienerowitz, M. Mazilu, and K. Dholakia, *J. Nanophotonics* **2**, 021875 (2008).

⁴M. Gu, J.-B. Haumonte, Y. Micheau, J. W. M. Chon, and X. Gan, *Appl. Phys. Lett.* **84**, 4236 (2004).

⁵P. C. Chaumet, A. Rahmani, and M. Nieto-Vesperinas, *Phys. Rev. Lett.* **88**, 123601 (2002).

⁶K. Okamoto and S. Kawata, *Phys. Rev. Lett.* **83**, 4534 (1999).

⁷H. X. Xu and M. Käll, *Phys. Rev. Lett.* **89**, 246802 (2002).

⁸G. Volpe, R. Quidant, G. Badenes, and D. Petrov, *Phys. Rev. Lett.* **96**, 238101 (2006).

⁹M. Righini, A. S. Zelenina, C. Girard, and R. Quidant, *Nat. Phys.* **3**, 477 (2007).

¹⁰A. N. Grigorenko, N. W. Roberts, M. R. Dickinson, and Y. Zhang, *Nat. Photonics* **2**, 365 (2008).

¹¹Z. Y. Fang, F. Lin, S. Huang, W. T. Song, and X. Zhu, *Appl. Phys. Lett.* **94**, 063306 (2009).

¹²M. Liu, T. Zentgraf, Y. M. Liu, G. Bartall, and X. Zhang, *Nature Nanotechnol.* **5**, 570 (2010).

¹³P. J. Reece, V. Garcés-Chavez, and K. Dholakia, *Appl. Phys. Lett.* **88**, 221116 (2006).

¹⁴M. Barth and O. Benson, *Appl. Phys. Lett.* **89**, 253114 (2006).

¹⁵D. M. Eigler and E. K. Schweizer, *Nature (London)* **344**, 524 (1990).

¹⁶C. Bustamante, Z. Bryant, and S. B. Smith, *Nature (London)* **421**, 423 (2003).

¹⁷P. Nordlander, C. Oubre, E. Prodan, K. Li, and M. I. Stockman, *Nano Lett.* **4**, 899 (2004).

¹⁸E. Prodan and P. Nordlander, *J. Chem. Phys.* **120**, 5444 (2004).

¹⁹F. M. Wang, H. Liu, T. Li, S. N. Zhu, and X. Zhang, *Phys. Rev. B* **76**, 075110 (2007).

²⁰H. Liu, D. A. Genov, D. M. Wu, Y. M. Liu, J. M. Steele, C. Sun, S. N. Zhu, and X. Zhang, *Phys. Rev. Lett.* **97**, 243902 (2006).

²¹N. Liu, H. Liu, S. N. Zhu, and H. Giessen, *Nat. Photonics* **3**, 157 (2009).

²²P. Nordlander and E. Prodan, *Nano Lett.* **4**, 2209 (2004).

²³J. L. Stratton, *Electromagnetic Theory* (McGraw-Hill, New York, 1941), Chap. 2.

²⁴B. Nikoobakht and M. A. El-Sayed, *Chem. Mater.* **15**, 1957 (2003).